Impact of Zn/Sn ion dual incorporation on the functional properties of electrospun PVP nanofibers for photovoltaic sensors

Y. O. Naif *, I. M. Ibrahim
University of Baghdad, College of Science, Department of Physics, Baghdad, Iraq

In this study, electrospun polyvinylpyrrolidone (PVP) nanofibers of varying Zn:Sn metal ion ratios were fabricated for optoelectronic applications. FESEM revealed reduced fiber diameter and connectivity when the Zn:Sn mixing ratio was increased. FTIR spectra exhibited characteristic PVP bands with slight shifts and intensity variations, along with the appearance of metal-oxygen bands. The thermal analysis indicates increasing the thermal stability with the added ions. Photovoltaic measurements showed that the Zn:Sn-mixed PVP fibres/n-type silicon exhibited a photovoltaic behavior, of 0.42% efficiency at a Zn:Sn ratio of 3:7. These results indicate the enhancement of co-ions-mixed PVP fibers for photovoltaic detectors.

(Received March 10, 2025; Accepted July 1, 2025)

Keywords: Electrospinning, Photodetector, PVP

1. Introduction

The synthesis and testing of electrospun polymer nanofibers have received considerable attention from researchers due to their unique structural, optical, and electrical properties [1]. Electrospun polymer nanofibers have gained significant attention due to their potential applications in various applications, including water filtration [2,3], tissue engineering [4], antibacterial applications [5], as well as optoelectronic fields [6]. Polyvinylpyrrolidone (PVP) is widely used among various polymer matrices due to its easy solubility, film formation ability, and compatibility with metal ions [7]. Incorporating metal ions into polymer nanofibers has been explored as a strategy to enhance their functional properties by rearranging the polymer chains and increasing the cohesion, improving the mobility of charge carriers, and increasing thermal stability [8]. The added metal ions improve the electronic structure of the polymer, making it more conductive [9] and modifying the structure and shape [10]. Photodetectors are electro-optical devices that convert optical signals into electrical signals. Photoelectric detectors are essential in optoelectronic applications [11].

Converting incident light into highly sensitive electrical signals [11]. They are essential in various modern technologies, such as optical communications, spectroscopy, biomedical imaging, and environmental sensors [12]. Integrating polymer nanofibers with metals is an approach to enhance light absorption, reduce charge carrier recombination losses, and improve charge carrier mobility [13,14]. Understanding the effect of metal ion doping on fiber morphology, thermal behavior, and electrical properties is crucial to optimizing these materials for device applications [15,16]. Several approaches are used to evaluate the thermal properties of polymers, including differential scanning calorimetry (DSC) and thermogravimetric analysis. TGA evaluates thermal behavior, including glass transition temperature (Tg) and crystallization points. These techniques help investigate the stability of the sample for use at different operating temperatures. This study explores the potential use of electrospun zinc-tin-enhanced polyvinylpyrrolidone (PVP) nanofibers as functional materials for photovoltaic energy detectors. By varying the zinc-tin ratio, we attempt to identify the optimal combination that balances electrical conductivity, structural properties, and thermal stability, thereby enhancing the performance of polymer-based photovoltaic energy detectors. The findings from this research will contribute to the development of advanced polymer-metal nanofiber fabrics with modified properties for polymer-based optoelectronics technologies.

* Corresponding author: yasir.udah2404m@sc.uobaghdad.edu.iq
https://doi.org/10.15251/JOR.2025.214.387

This study explores the effect of a dual mix of Zn/Sn ions with the electrospun PVP nanofibers at varying Zn:Sn ratios for photovoltaic detectors. The investigation on the optimal Zn:Sn composition ratio enhances electrical, structural characteristics, and thermal stability and improves the performance of polymer-based photovoltaic detectors.

2. Experimental setup

Polyvinylpyrrolidone (PVP), Tin acetate ($Sn(CH_3CO_2)_2$), and zinc acetate ($Zn(CH_3CO_2)_2$) from (Sigma-Aldrich Co.) were utilized as starting substances. 1gm of PVP was dissolved in 12 ml of 70% ethanol: water solution under stirring for 4 hours at room temperature. Tin and zinc acetates were dissolved in 70% ethanol: water solution at 0.2 M concentration. The metal acetate solution was mixed together in 1:0, 3:1, and 1:1 Sn:Zn ions ratios. The metal ions solution combined with the PVP solution at 3:7 on a magnetic stirrer for 40 minutes resulted in 0.06 M of metal ions in the final polymer solutions and the pure PVP sample. The flow rate of the syringe pump was adjusted at 0.5 ml/h. The needle-to-collector distance was fixed at 12 cm. A voltage difference of 20 kV was applied. The structural, surface morphology, molecular bands, and thermal properties were examined.

The photovoltaic sensor in the Al/n-Si/(Zn, Sn):PVP fiber/Al structure is connected by thin wires using silver paste with the grid of Al on the top of the reinforced-PVP fiber fabric during the connection of the entire back deposit by aluminum. The I-V characteristics were examined under dark and white light conditions of 100 mw/cm^2 intensity.

3. Results and discussions

Figure 3 presents the XRD patterns of as deposited- PVP nanofibers on glass substrates, compared with samples incorporating Zn and Sn ions at varying Zn/Sn ratios. The pristine PVP fiber exhibits a wide broad hump, indicating its amorphous nature, which is consistent with previously reported studies [17]. Upon the introduction of Sn ions in sample (b), two distinct diffraction peaks emerge at approximately $2\theta \approx 14°$ and 17°. The presence of these peaks denotes increased structural organization within the PVP matrix, likely due to ionic interactions promoting chain alignment by localized ordering. The dual mixing of Zn and Sn ions at the 1:3 ratio enhances the intensity of these diffraction peaks. It is enhanced by increasing the Zn/Sn ratio to 1:1. The increase in peak intensity indicates a transition towards a more ordered phase.

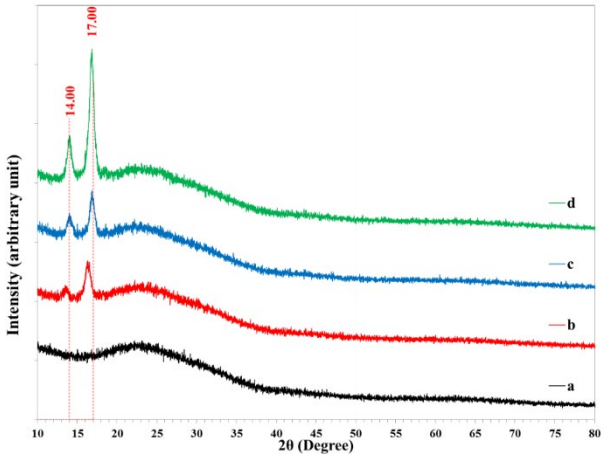

Fig. 1. XRD patterns of the electrospun (a) PVP fiber, (b) mixed with Sn ions, (c)combined with Zn:Sn ions at 1:3, and (d) 1:1 ratios.

The added ions enhance PVP molecular arrangement through intermolecular interactions. This result suggests the influence of ionic incorporation on the structural properties of PVP nanofibers, which could have implications for the electrospun PVP nanofibers in a wide range of applications.

Figure 2 shows the FE-SEM images at two magnifications, along with the fiber diameter distribution histograms, providing a detailed analysis of the morphological changes in electrospun PVP nanofibers upon incorporating Sn and Zn ions. The pure PVP nanofibers exhibit a relatively uniform structure of broad size distribution, from 100 to 400 nm, with an average diameter of 179.40 nm. The fiber fabric appears smooth and continuous with low connectivity.

Incorporating Sn ions into the PVP matrix causes significant decreases in fiber diameter to an average of 81.40 nm. The nanofibers appeared more tightly packed than pure PVP. The fiber diameter distribution becomes narrower, indicating more uniformity. The reduction in fiber diameter with Sn ions results from variation in the viscosity of the injected polymer solution. The dual addition of Zn:Sn at a 1:3 atomic ratio increases the average fiber diameter to 136.88 nm. The fiber network appears more interconnected, with some structural irregularities. A broader diameter distribution appears than Sn-doped nanofibers, suggesting that including Zn ions affects the fiber formation.

The sample with a 1:1 Zn:Sn ratio exhibits the thinnest fiber diameter, with an average diameter of 71.58 nm. The distribution appears more uniform and more packed than other samples. The histogram confirms a narrower size distribution, indicating improved consistency in fiber formation. The balanced incorporation of Zn and Sn ions in equal proportions likely optimizes metal-polymer interactions and enhances connectivity, benefitting electrical and optoelectronic applications.

The observed variations in fiber morphology highlight the impact of metal ion doping on electrospun PVP nanofibers. The reduction in fiber diameter upon doping suggests that metal ions influence polymer solution properties, particularly in controlling fiber formation during electrospinning. The observed dotted nanofibers in the Zn:Sn (1:1) sample suggest the formation of a zinc-rich polymer matrix. These dots, likely metal oxide nanoparticles, interact strongly with the PVP structure, leading to localized phase separation.

Figure (3) displays the Fourier Transform Infrared (FTIR) spectra of the electrospun PVP nanofibers and the Zn/Sn-mixed fiber samples at different Zn/Sn ratios. The PVP fiber spectrum displays the characteristic absorption bands associated with the PVP polymer functional groups, as shown in. A broad absorption band around 3400 cm^{-1} corresponds to the stretching vibration of hydroxyl (-OH) groups, which can be attributed to the residual solvent. Strong peaks around 2920 and 2850 cm^{-1} correspond to the stretching vibrations of C-H bonds in the polymer backbone [18]. The characteristic C=O stretching of the amide group in PVP appears at approximately 1650 cm^{-1}, while the C-N and C-O stretching vibrations are evident at around 1280 and 1030 cm^{-1}, respectively [19].

The Sn ion-mixed fiber samples display notable changes in the FTIR pattern of PVP, indicating chemical interactions between the polymer matrix and the introduced metal ions, as well as emerging new bands. The hydroxyl (-OH) stretching band shifts slightly, indicating interactions between Sn^{4+} and the oxygen-containing functional groups in PVP [20]. Additionally, the characteristic C=O band displays a slight shift and intensity difference, suggesting the formation of bonds between the added Sn^{4+} ion and the polymer's carbonyl groups. The additional bands around 650 and 580 cm^{-1} match the Sn-O-Sn and Sn-O vibrations, confirming the presence of SnO_2 [21]. The PVP nanofibers reinforced with Zn:Sn at a ratio of 1:3 show shape changes in the PVP vibration bands. The intensity of the C=O stretching vibration decreases slightly, indicating a more pronounced interaction between the metal ions and the functional groups of the polymer. The spectrum proves the presence of the Zn-O bond by the broad vibration band that appeared at about 500 cm^{-1} [22]. Further modifications are observed at the 1:1 Zn:Sn ratio. The -OH stretching band broadens, suggesting stronger hydrogen bonding and coordination interactions with metal ions. The C=O band at 1650 cm^{-1} undergoes a more noticeable shift, and the intensities of the C-N and C-O bands at 1280 and 1030 cm^{-1} also change, indicating enhanced metal-polymer interactions. The peaks corresponding to Sn-O and Zn-O become more distinct, confirming the formation of a well-integrated Zn/Sn-oxide phase within the polymer matrix. Table (1) lists the electrospun PVP

fiber's FTIR bands and that mixed with Zn and Sn acetates at different Zn/Sn ratios.

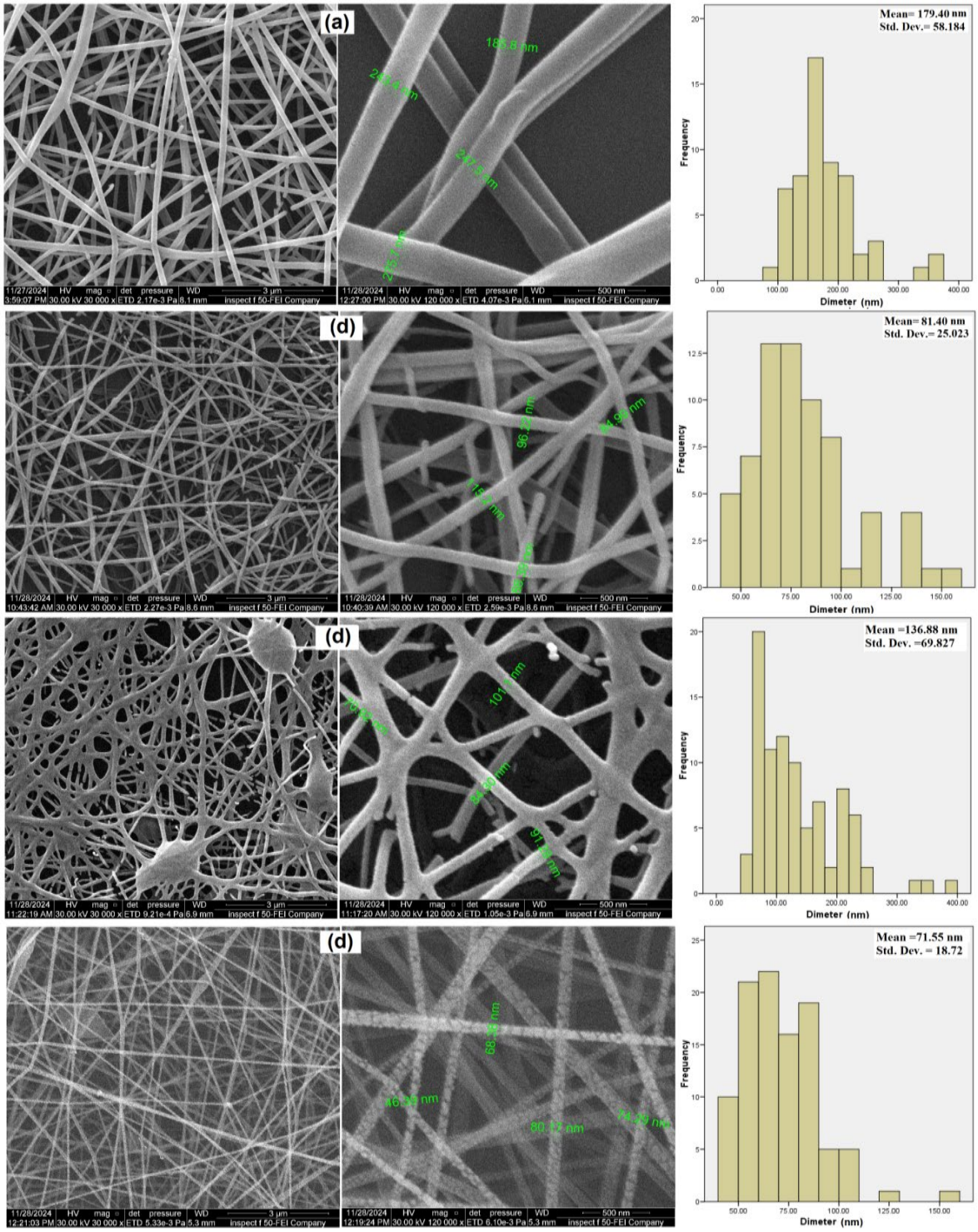

Fig. 2. FE-SEM images and fiber diameter distribution histogram of electrospun (a) PVP fiber, (b) mixed with Sn ions, (c) combined with Zn:Sn ions at 1:3, and (d) 1:1 ratios.

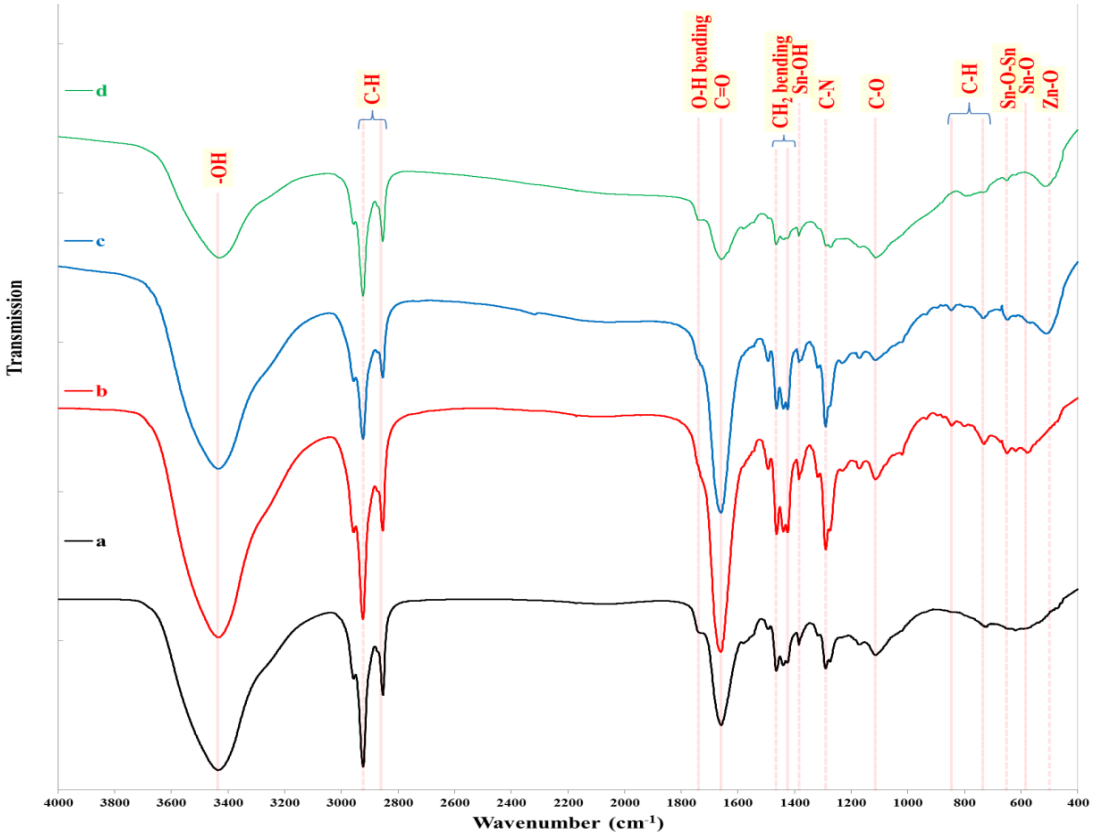

Fig. 3. FTIR spectra of electrospun (a) PVP fiber, (b) mixed with Sn ions, (c) combined with Zn:Sn ions at 1:3, and (d) 1:1 ratios.

Table 1. FTIR bands of electrospun (a) PVP fiber, (b) mixed with Sn ions, (c) combined with Zn:Sn ions at 1:3, and (d) 1:1 ratios.

Band Type	PVP	with Sn ions	1:3 of Zn:Sn	1:1 of Zn:Sn
-OH	3436.73	3436.16	3435.74	3430.87
C-H stretch	2923.25	2923.94	2923.51	2923.59
	2853.16	2853.78	2853.62	2853.33
O-H bending	1730.00	-	-	1730.00
C=O	1659.26	1660.33	1659.36	1658.52
CH_2 bending	1464.16	1463.45	1463.46	1464.92
	1425.08	1424.48	1424.51	-
Sn-OH	1384.77	1384.65	1384.09	1384.82
C-N	1290.27	1290.00	1290.45	-
C-O	1114.03	1114.19	1113.82	1113.63
C-H	-	845.67	846.81	792.94
	720.89	731.07	732.17	-
Sn-O-Sn	-	650.41	647.26	651.33
Sn-O	-	585.99	579.12	-
Zn-O	-	-	500.12	490.00

The thermal behavior of electrospun PVP nanofibers and the metal ions-reinforced samples were analyzed through Differential Scanning Calorimetry (DSC) and Differential Thermal Analysis (DTA), as shown in Figure (4). The DSC curves of pure PVP nanofibers exhibit an initial endothermic peak around 64.2°C, corresponding to the moisture loss. As the temperature increases, a significant decomposition peak appears at approximately 433.6°C, indicating polymer

degradation. A secondary degradation step occurs around 500.0 °C, corresponding to the degradation of remaining organic fractions [23].

When Sn ions are introduced into the PVP matrix, the DSC curve slightly shifts the decomposition temperature to 437.1°C. This shift to a higher temperature indicates that Sn ions contribute to the improved thermal stability of the nanofibers. An additional peak at 560.7°C in the DTA curve indicates a secondary degradation process, likely linked to interactions between Sn ions and the polymer network, possibly forming a more thermally resistant structure. For PVP nanofibers reinforced with Zn:Sn ions at a 1:3 ratio, the DSC analysis reveals a similar moisture loss region below 100°C. The DTA curve at 436.8°C determines the decomposition peak. The secondary degradation peak in the DTA curve at 561.0°C is more pronounced, implying that the Zn:Sn combination further alters the polymer's thermal degradation due to forming Zn-O and Sn-O bonds with the polymer functional groups. The thermal profile of the PVP nanofibers containing Zn:Sn at a 1:1 ratio presents the most significant shift in thermal stability. The initial moisture loss occurs, followed by a decomposition peak at 438.1°C, the highest among all samples. The DTA curve reveals an additional transformation at 754.4°C, which is not observed in the other samples. This peak is likely associated with the crystallization or oxidation of metal ions into stable oxides, further enhancing the material's thermal resistance, where zinc has the highest oxidizing capability compared with other metals.

The enhanced thermal stability of PVP nanofiber fabric mixed with a balanced ratio of the two ions can be attributed to their distinct interactions with the polymer matrix. Tin ions (Sn^{4+}) exhibit a strong affinity for the oxygen-containing functional groups in PVP, such as carbonyl (-C=O) and hydroxyl (-OH) groups. This interaction results in the formation of coordination bonds, which lead to increased crosslinking within the polymer network.

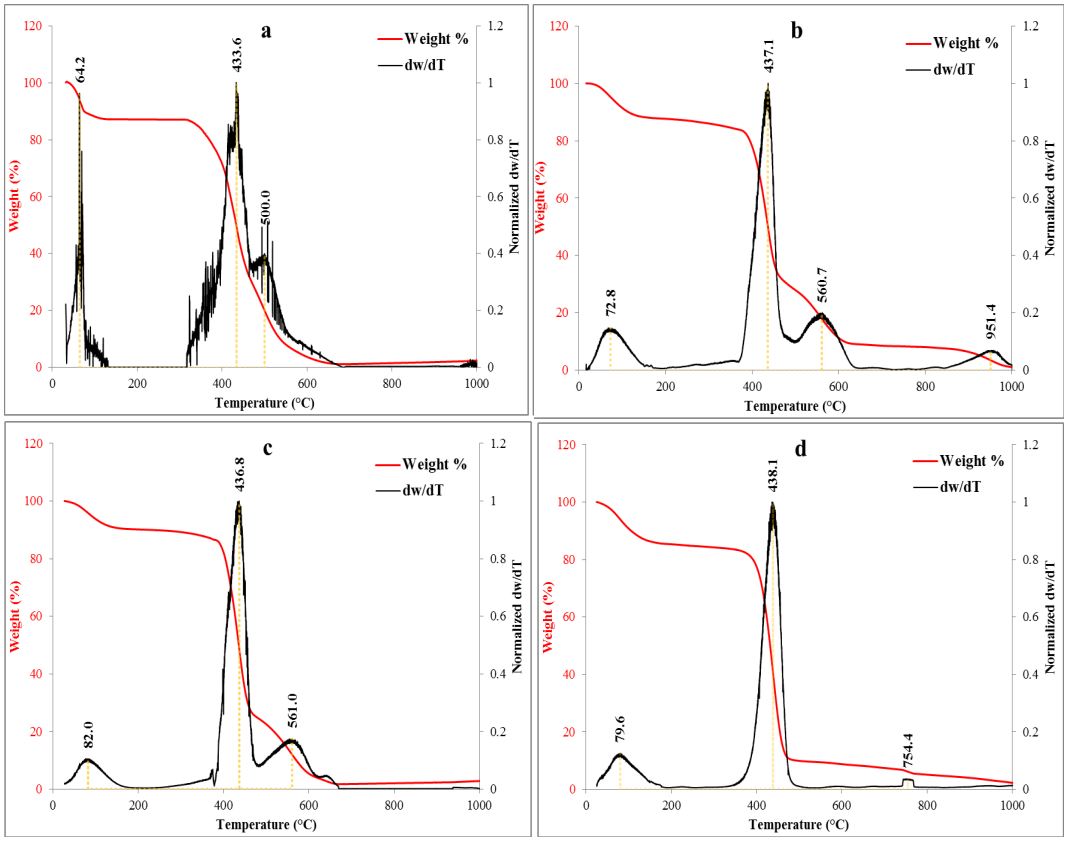

Fig. 4. DSC and DTA test of electrospun (a) PVP fiber, (b) mixed with Sn ions, (c) combined with Zn:Sn ions at 1:3, and (d) 1:1 ratio.

As a result, the polymer becomes more rigid at a specific ratio, contributing to higher thermal resistance. In contrast, zinc ions (Zn^{2+}) interact with PVP through weaker ionic interactions, forming Zn–O bonds with polymer functional groups. The resulting crosslinking is less extensive. However, Zn^{2+} plays a crucial role in stabilizing the polymer by forming ZnO nanoparticles, which help dissipate heat and reduce the polymer degradation rate at high temperatures. Combining Zn^{2+} and Sn^{4+} in a 1:1 ratio enhances an optimal balance by providing the ideal balance between crosslinking and flexibility.

The thermogravimetric analysis (TGA) of the electrospun PVP and its Zn/Sn-mixed samples at different ratios provides their thermal transitions, including the glass transition temperature (Tg) and crystalline temperature (Tc), as shown in Figure 5

The pure PVP sample exhibits a glass transition temperature of around 74.7°C, corresponding to the polymer matrix's softening. This peak becomes indistinct after the incorporation of metal ions. The interaction between the metal ions and PVP chains disrupts the transition clarity of the Tg. The complexation of metal ions with PVP may increase crosslinking or rigidity, leading to a loss of a well-defined glass transition behavior.

In samples PVP:Sn and at Zn:Sn of 1:3, two distinct exothermic peaks, one around 460°C and another around 577°C [24]. The appearance of two peaks may also indicate phase separation, so the existence of multiple crystalline phases within the material, each with different thermal stability. Some regions of the polymer may exhibit weaker metal coordination, leading to earlier degradation, while other areas with stronger metal coordination remain stable at higher temperatures. The second peak may be associated with the interaction of metal ions, such as a metal-oxide bond with the polymer, causing crystallization at elevated temperatures.

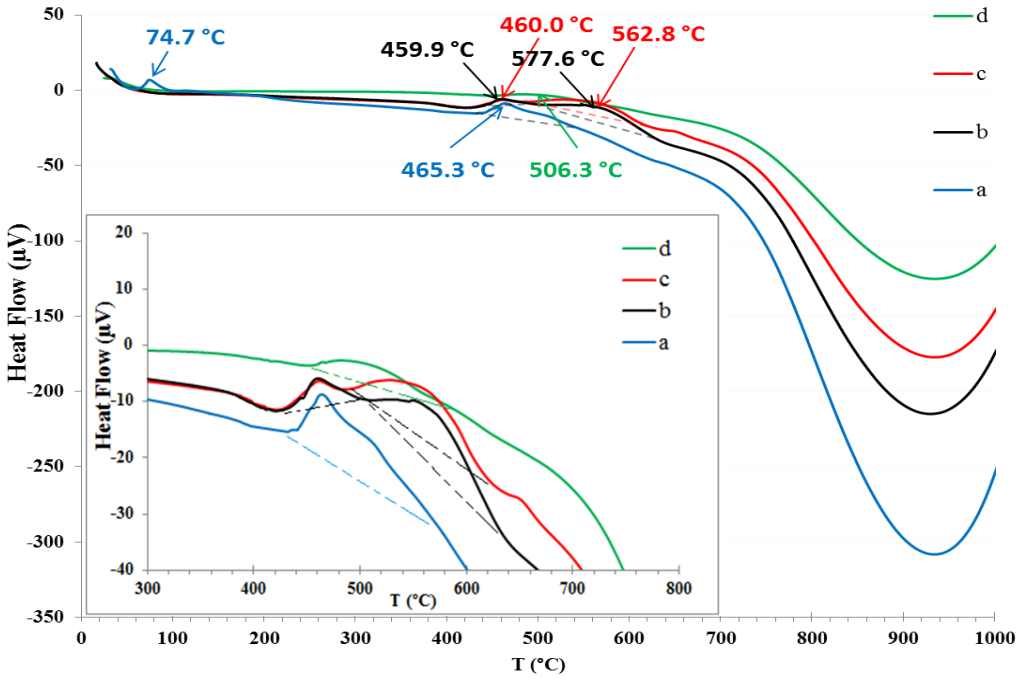

Fig. 5. TGA test of electrospun (a) PVP fiber, (b) mixed with Sn ions, (c) combined with Zn:Sn ions at 1:3, and (d) 1:1 ratio.

The Seebeck effect refers to the possibility of creating a current from a temperature gradient [25]. Figure 6 displays the determination of the Seebeck coefficient of PVP fiber mixed with Sn ions, Zn:Sn ions at 1:3, and 1:1 ratio. Seebeck coefficient (S) equals the slope of the relationship between voltage (V) and temperature gradient (ΔT). The S value determines thermoelectric efficiency. The R^2 values larger than 0.9 for all samples indicate the confidence of the results.

The pure PVP nanofibers exhibit the highest Seebeck coefficient, with S= 68.742 μV/K. The PVP structure possesses a thermoelectric response due to its polymer chain alignment and charge carrier mobility. S value decreases to 55.511 μV/K for Sn ions-mixed PVP. The presence of Sn ions alters the charge transport pathways, likely increasing electrical conductivity but reducing the overall thermoelectric voltage generation. The formation of SnO_2 within the polymer matrix may contribute to these changes by modifying carrier density and reducing thermal conductivity. When a Zn:Sn ion ratio of 1:3 is incorporated into the PVP nanofibers, the Seebeck coefficient further declines to 46.785 μV/K, due to a higher charge carrier concentration, leading to improved electrical conductivity but a reduction in the thermoelectric effect. The dominant SnO_2 phase within the polymer network appears to influence carriers' mobility.

In the case of PVP nanofibers reinforced with a Zn:Sn ratio of 1:1, the Seebeck coefficient improves slightly to 51.125 μV/K. This indicates a balance between charge carrier mobility and concentration. The co-presence of Zn and Sn ions likely enhances charge transport while maintaining moderate thermoelectric performance.

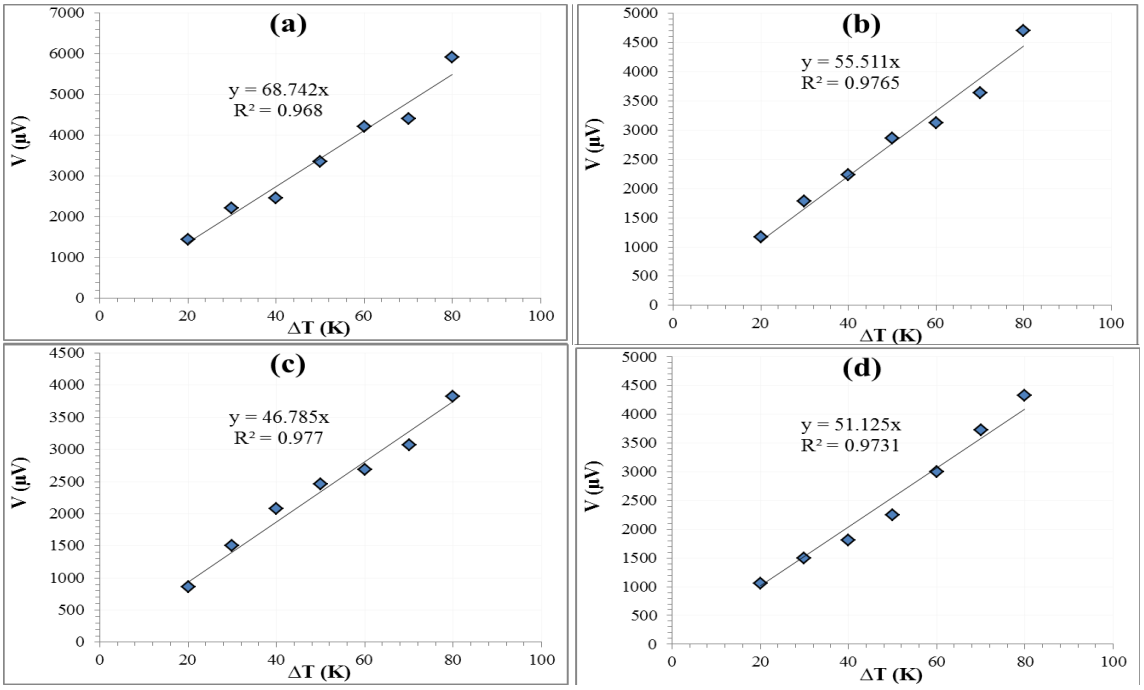

Fig. 6. Seebeck test of electrospun (a) PVP fiber, (b) mixed with Sn ions, (c) combined with Zn:Sn ions at 1:3, and (d) 1:1 ratio.

The I-V characteristics of the electrospun PVP nanofibers and their Zn/Sn- reinforced sample on n-type Si wafers in dark and white light conditions, shown in Figure (7), reveal distinct photovoltaic potential. The I-V curves provide numerous parameters, including short-circuit current (Isc), open-circuit voltage (V_{oc}), maximum current (I_m), maximum voltage (V_m), fill factor (FF), and efficiency. The ideality factor (β) was determined from the slope of ln(I) versus V at low bias voltage, as shown in Figure 8, which determined the enhancement of charge transport and diode performance. The table lists the photovoltaic parameters of electrospun PVP fiber mixed with Sn ions, Zn:Sn ions at 1:3, and 1:1 ratio on n-Si. The PVP fiber sample exhibits the lowest photovoltaic efficiency of 0.05%, with Isc = 0.80 mA and V_{oc} = 0.20 V. The fill factor (FF) is 0.33, and the ideality factor β = 3.31, indicating high recombination losses. The poor photovoltaic performance is attributed to the insulating nature of PVP, which lacks sufficient charge carrier mobility. Composing with Sn ions enhances performance, increasing I_{sc} to 2.62 mA and V_{oc} to 0.50 V, leading to a higher efficiency of 0.40%, with a better fill factor and ideality factor. Incorporating Sn ions may improve charge carrier separation and reduce recombination losses by modifying the polymer connectivity and reducing charge trapping. The 1:3 of Zn:Sn results in the highest I_{sc} and V_{oc}, achieving the best efficiency of 0.42%. This enhancement is attributed to the

dual effect of Zn and Sn ions, which optimize the electrical conductivity. A 1:1 Zn:Sn ratio leads to an efficiency of 0.19% and an ideality factor of 2.15, indicating moderate recombination losses. The performance is lower than the 1:3 Zn:Sn ratio sample, suggesting that a higher Sn concentration than Zn ions favors better charge transport and photovoltaic response.

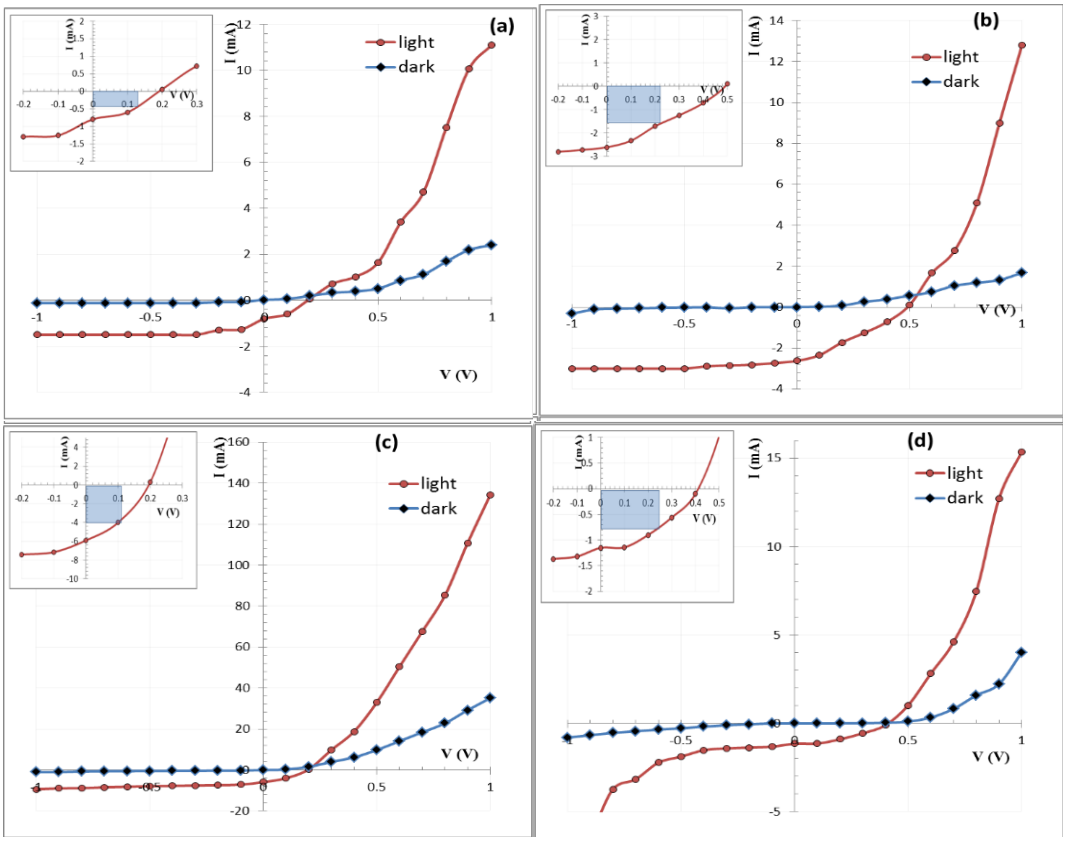

Fig. 7. I-V characteristics of electrospun (a) PVP fiber, (b) mixed with Sn ions, (c) combined with Zn:Sn ions at 1:3, and (d) 1:1 ratio on n-Si.

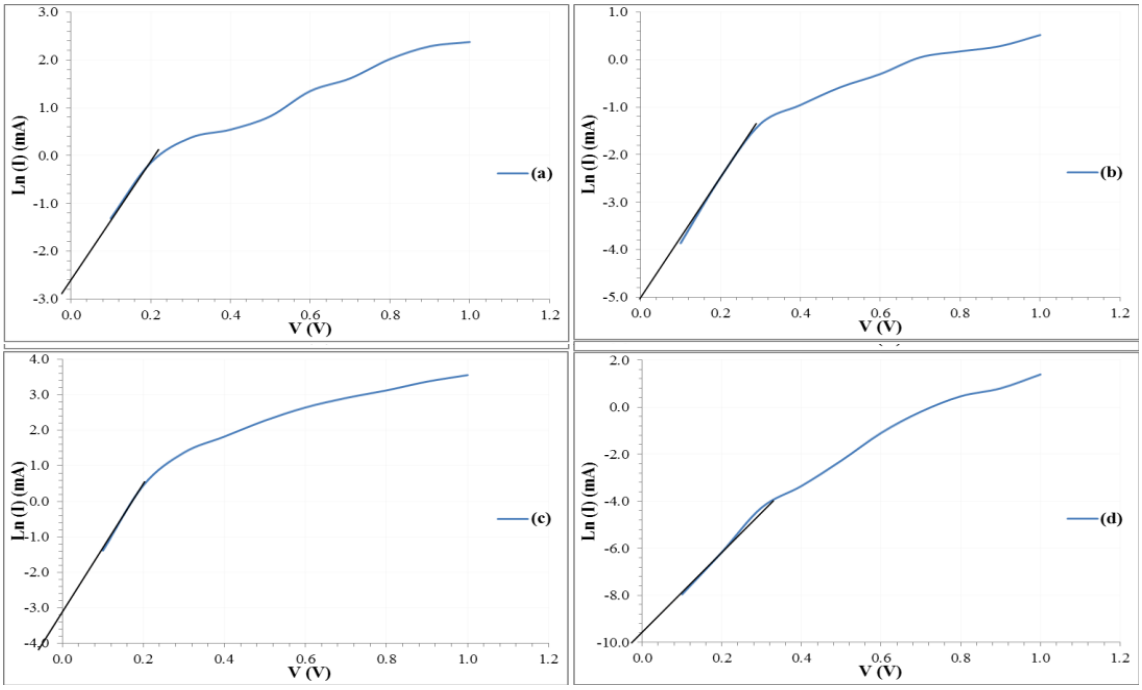

Fig. 8. Ln(I) versus V of electrospun (a) PVP fiber, (b) mixed with Sn ions, (c) combined with Zn:Sn ions at 1:3, and (d) 1:1 ratio.

Table 2. Photovoltaic parameters of electrospun PVP fiber, mixed with Sn ions, Zn:Sn ions at 1:3, and 1:1 ratio on n-Si.

Sample	Isc (mA)	Voc(V)	Im (mA)	Vm (V)	FF	Efficiency %	β
PVP	0.80	0.20	0.40	0.13	0.33	0.05	3.31
PVP: Sn/n-Si	2.62	0.50	1.60	0.25	0.31	0.40	2.77
PVP:$(Zn)_1(Sn)_3$/n-Si	6.00	0.20	3.50	0.12	0.35	0.42	2.09
PVP:$(Zn)_1(Sn)_1$/n-Si	1.15	0.40	0.80	0.24	0.42	0.19	2.15

4. Conclusions

This study displays the potential of dual Zn and Sn ion-reinforced electrospun PVP nanofibers for photovoltaic sensor applications. The balance of the two ions improves thermal, mechanical, and optoelectronic properties. The crystallinity of the polymer composite is improved with the combined Zn-Sn ion incorporation, which is further confirmed by SEM images, revealing that the controlled incorporation of Zn and Sn ions ratio leads to a significant reduction in fiber diameters, enhanced fiber connectivity in metal-doped samples suggests potential improvements in electrical and optoelectronic performance. FTIR analysis demonstrates that introducing Zn^{2+} and Sn^{4+} ions into PVP nanofibers alters polymer functional group interactions. The observed shifts in key IR bands and the appearance of metal-oxygen vibrations confirm successful reinforcing with the Zn:Sn (1:1) sample.

Thermal analysis through DSC and DTA reveals that reinforcing with Zn and Sn ions significantly impacts the thermal stability of PVP nanofibers. The shift in decomposition temperatures and the emergence of new thermal events. The Zn:Sn (1:1) sample exhibits the highest thermal stability, making it a promising material for thermally stable applications. Additionally, the disappearance of the T_g peak after metal ion incorporation suggests restricted polymer chain movement due to strong polymer-metal interactions. The two-step decomposition process indicates the presence of multiple thermal phases. In addition, the reinforcing by the dual Zn and Sn ions significantly influences the Seebeck coefficient of the PVP fibers. Adding metal ions improves electrical conductivity, especially with the Zn:Sn (1:1) ratio.

The photovoltaic performance indicates that the combined reinforcement of PVP nanofibers by Zn and Sn ions enhances the efficiency of PVP/n-Si heterojunction. The highest photovoltaic efficiency of 0.42% is achieved with a Zn:Sn ratio of 1:3 by enhancing charge carrier mobility and minimizing recombination losses. The overall results indicate the promising use of the prepared nanofibers for optoelectronic applications.

References

[1] M. S. A. Hamid and I. M. Ibrahim, Iraqi J. Appl. Phys. 20, 687 (2024).

[2] S. Nur'aini, A. Zulfi, B. H. Arrosyid, A. F. Rafryanto, A. Noviyanto, D. A. Hapidin, D. Feriyanto, K. E. Saputro, K. Khairurrijal, N. T. Rochman, RSC Adv. 12, 33751 (2022); https://doi.org/10.1039/D2RA05969J

[3] F. J. Hameed and I. M. Ibrahim, J. Ovonic Res. 20, 525 (2024); https://doi.org/10.15251/JOR.2024.204.525

[4] M. Sohrabi, M. Abbasi, M. M. Ansar, B. Soltani Tehrani, Polym. Bull. 79, 8397 (2022); https://doi.org/10.1007/s00289-021-03905-5

[5] K. N. Narasimhamurthy, B. Daruka Prasad, B. R. Radha Krushna, S. C. Sharma, K. Ponnazhagan, D. Francis, T. B. Nijalingappa, M. Nasreen Taj, H. Nagabhushana, Inorg. Chem. Commun. 156, 111161 (2023); https://doi.org/10.1016/j.inoche.2023.111161

[6] S. Kailasa, M. S. B. Reddy, M. R. Maurya, B. G. Rani, K. V. Rao, K. K. Sadasivuni, Macromol. Mater. Eng. 306, 2100410 (2021); https://doi.org/10.1002/mame.202100410

[7] M. Teodorescu, M. Bercea, Polym. - Plast. Technol. Eng. 54, 923 (2015); https://doi.org/10.1080/03602559.2014.979506

[8] X. Chen, H. Cao, Y. He, Q. Zhou, Z. Li, W. Wang, Y. He, G. Tao, C. Hou, Front. Optoelectron. 15, 1 (2022); https://doi.org/10.1007/s12200-022-00051-2

[9] S. H. Abdullah, M. O. Salman, H. R. Humud, Karbala Int. J. Mod. Sci. 5, 145 (2019); https://doi.org/10.33640/2405-609X.1138

[10] Y. Wang, T. Yokota, T. Someya, NPG Asia Mater. 13, (2021); https://doi.org/10.1038/s41427-020-00267-8

[11] X. Hu, X. Li, G. Li, T. Ji, F. Ai, J. Wu, E. Ha, J. Hu, Adv. Funct. Mater. 31, (2021); https://doi.org/10.1002/adfm.202011284

[12] A. Qadir, S. Shafique, T. Iqbal, H. Ali, L. Xin, S. Ruibing, T. Shi, H. Xu, Y. Wang, Z. Hu, Sensors Actuators A Phys. 370, 115267 (2024); https://doi.org/10.1016/j.sna.2024.115267

[13] M. J. Tommalieh, N. S. Awwad, H. A. Ibrahium, A. A. Menazea, Radiat. Phys. Chem. 179, 109195 (2021); https://doi.org/10.1016/j.radphyschem.2020.109195

[14] S. A. Hamdan, Iraqi J. Sci. 65, 2479 (2024); https://doi.org/10.24996/ijs.2024.65.5.12

[15] F. Cao, W. Tian, B. Gu, Y. Ma, H. Lu, L. Li, Nano Res. 10, 2244 (2017); https://doi.org/10.1007/s12274-016-1413-2

[16] M. J. Hamadamin, N. K. Hassan, M. Humayun, M. Bououdina, J. Photochem. Photobiol. A Chem. 459, 116017 (2025); https://doi.org/10.1016/j.jphotochem.2024.116017

[17] X. Zhang, Y. Yang, Z. Li, X. Liu, C. Zhang, S. Peng, J. Han, H. Zhou, J. Gou, F. Xiu, J. Wang, Adv. Opt. Mater. 9, 1 (2021).

[18] K. Jeyabanu, K. Sundaramahalingam, P. Devendran, A. Manikandan, N. Nallamuthu, Phys. B Condens. Matter 572, 129 (2019); https://doi.org/10.1016/j.physb.2019.07.049

[19] H. E. Ali, H. S. M. Abd-Rabboh, N. S. Awwad, H. Algarni, M. A. Sayed, A. F. A. El-Rehim, M. M. Abdel-Aziz, Y. Khairy, Optik (Stuttg). 247, 167863 (2021); https://doi.org/10.1016/j.ijleo.2021.167863

[20] M. Teodorescu, M. Bercea, S. Morariu, Biotechnol. Adv. 37, 109 (2019); https://doi.org/10.1016/j.biotechadv.2018.11.008

[21] V. Siva, D. Vanitha, A. Murugan, A. Shameem, S. A. Bahadur, Compos. Commun. 23,

100597 (2021); https://doi.org/10.1016/j.coco.2020.100597

[22] D. Xiang, F. Qu, X. Chen, Z. Yu, L. Cui, X. Zhang, J. Jiang, H. Lin, J. Sol-Gel Sci. Technol. 69, 370 (2014); https://doi.org/10.1007/s10971-013-3229-9

[23] P. Singh, D. C. Bharati, P. N. Gupta, A. L. Saroj, J. Non. Cryst. Solids 494, 21 (2018); https://doi.org/10.1016/j.jnoncrysol.2018.04.052

[24] M. T. Razzak, Zainuddin, Erizal, S. P. Dewi, H. Lely, E. Taty, Sukirno, Radiat. Phys. Chem. 55, 153 (1999); https://doi.org/10.1016/S0969-806X(98)00320-X

[25] Z. U. Khan, J. Edberg, M. M. Hamedi, R. Gabrielsson, H. Granberg, L. Wågberg, I. Engquist, M. Berggren, X. Crispin, Adv. Mater. 28, 4556 (2016); https://doi.org/10.1002/adma.201505364